Available online at www.sciencedirect.com
SCIENCE DIRECT®
ELSEVIER
Journal of Sound and Vibration 285 (2005) 967–987
JOURNAL OF SOUND AND VIBRATION
www.elsevier.com/locate/jsvi

Crack identification in beam from dynamic responses

S.S. Law*, Z.R. Lu

Civil and Structural Engineering Department, The Hong Kong Polytechnic University, Hunghom, Kowloon, Hong Kong, People's Republic of China

Received 20 September 2003; received in revised form 3 September 2004; accepted 10 September 2004
Available online 1 January 2005

Abstract

A time domain method is proposed in which the parameters of a crack in a structural member are identified from strain or displacement measurements. The crack is modeled as a discrete open crack represented mathematically by the Dirac delta function. The dynamic responses are calculated basing on modal superposition. In the inverse analysis, optimization technique coupled with regularization on the solution is used to identify the crack(s). The formulation for identification is further extended to the case of multiple cracks. A general orthogonal polynomial function is used to generate the derivatives of the strain or displacement time responses to eliminate the error due to measurement noise. Computation simulations with sinusoidal and impulsive excitations on a beam with a single crack or multiple cracks show that the method is effective for identifying the crack parameters with accuracy. The proposed identification algorithm was also verified experimentally from impact hammer tests on a beam with a single crack.

1. Introduction

Inspection of the structural components for damage is important for making decision on the maintenance program of the structure. System identification is an important tool in the dynamic identification for such purpose. It has gained increasing attention from the scientific community and there has been a lot of research in the last two decades. A lot of work has been published in the area of damage detection and a variety of methods has been developed. These methods are

*Corresponding author. Tel.: +852 2766 6062; fax: +852 2334 6389.
E-mail address: cesslaw@polyu.edu.hk (S.S. Law).

0022-460X/$ - see front matter
doi:10.1016/j.jsv.2004.09.036

Nomenclature

ρ	mass density of the beam material
A	cross-sectional area
h_0	the height of the beam
b	the width of the beam
c	the viscous damping of the beam
$P(t)$	the external exciting force
E	Young's modulus
I_0	the moment of inertia of the beam cross-section
I_d	the moment of inertia of the beam cross-section at the crack
T	kinetic energy of the beam
U	strain energy
W	work done due to the external force
W_c	work done due to the viscous damping
$y(x,t)$	transverse displacement of the beam
$Y_i(x)$	the ith mode shape of the beam
$q_i(t)$	modal coordinate
M	modal mass matrix
C	modal damping matrix
K	modal stiffness matrix
K'	modal stiffness loss due to the crack
N	number of modes used
N_f	number of the polynomial terms used
λ	regularization parameter

mainly based on the relationship between the dynamic characteristics, such as the natural frequencies [1,2] or mode shapes [3] and the damage parameters like the crack depth and its location. It is noted that the presence of a crack in a structural member introduces a local flexibility affecting its responses to load.

A variety of crack models can be found in the literature modeled as a spring [1,4], an elastic hinge [3,5], a cut-out slot [6], a pair of concentrated moment couple [7,8], a zone with a reduced Young's modulus [9], or mathematically, as a semi-empirical damage function describing the stress and strain distribution in the volume of the cracked beam [10,11]. The crack has also been modeled as a spring with bilinear stiffness [12]. Crack function models were also developed [13] to model the crack in more details. Recent researches in this area also include beams with breathing cracks [2] and the modeling on the nonlinearity of a beam with a number of breathing cracks [14].

Most of the damage identification problems are solved in the frequency domain. Change in natural frequencies is one of the "classical" damage indicators. Cawley and Adams [15] are among the first ones to detect damage in elastic structure by using natural frequencies. On the basis of changes in the natural frequencies, Messina et al. [16] calculated the Damage Location Assurance Criterion, which was used to identify single defect and was later extended to identify multiple damage sites [17]. Also many publications have used the mode shape measurements to detect damage. Pandey et al. [18] used complete mode shapes from the undamaged and damaged states to identify both the location and the extent of damage by solving a system of linear equations. Shi and Law [19] calculated the modal strain energy change before and after the occurrence of damage as indicator to identify damage. These methods need information from the measured mode shapes.

More recently damage detection in time domain has been studied by several researchers. Cattarius and Inman [20] used the time histories of vibration response of the structure to identify damage in smart structures. Koh et al. [21] studied the structural stiffness parameters of a multi-storey framework in a system identification approach. Majumder and Manohar [22] made use of the excitation from passing vehicles on top of a bridge beam for the damage detection in beam structures.

The present study explicitly includes the crack damage in the identification equation of a beam structure. A crack with a constant depth is modeled with a Dirac delta function, and a method is proposed to identify the crack parameters using the dynamic responses. The method is developed based on the modal superposition and optimization technique in combination with regularization on the solutions to smooth out the large variations in the identified results. Either the displacement or the strain measurement can be used to identify the crack, and only the first few modes from several measuring points are required for the identification. Identification of both the single crack and multiple cracks are studied numerically with sinusoidal or impulsive excitation. The identification algorithm is later verified using experimental results from a beam with a single crack.

2. Direct problem

2.1. Equations of motion

A single-span uniform Euler–Bernoulli beam with a single-sided transverse crack subjected to an excitation force $P(t)$ acting at x_p from the left support is shown in Fig. 1. The crack is assumed to be fully open and has a fixed depth h_c at a location distant x_c from the left support. The equation of motion of the beam can be written as

$$\rho A \frac{\partial^2 y(x,t)}{\partial t^2} + c\frac{\partial y(x,t)}{\partial t} + (EI_0 - EI_c\delta(x-x_c))\frac{\partial^2}{\partial x^2}\left(\frac{\partial^2 y(x,t)}{\partial x^2}\right) = P(t)\delta(x-x_p), \tag{1}$$

where ρ is the mass density of the beam, A is the cross-sectional area, c is the damping of the beam, E is the Young's modulus of material, I_0 is the moment of inertia of the beam cross-section, I_c is the reduction of the moment of inertia of beam cross-section at the crack defined as $b/12[h_0^3 - (h_0 - h_c)^3]$, $y(x,t)$ is the transverse displacement function of the beam, $\delta(x)$ is the Dirac delta function and b is the width of the beam. The beam is assumed to be at rest at the beginning of the identification, and the damping effect originated from the crack is not considered.

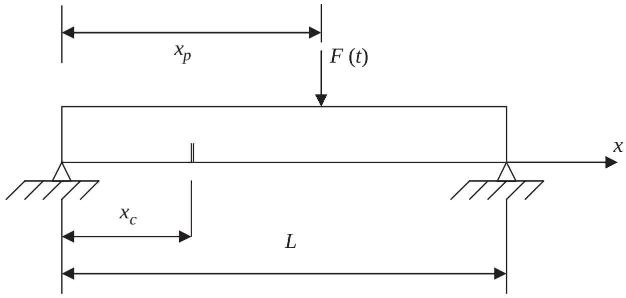

Fig. 1. The cracked beam model.

The kinetic energy T, the strain energy U, the work done W_c due to the viscous damping in the beam, and the work done W due to the external force can be expressed as

$$T = \frac{1}{2}\int_0^L \rho A \left(\frac{\partial y(x,t)}{\partial t}\right)^2 \mathrm{d}x, \tag{2}$$

$$U = \frac{1}{2}\int_0^L EI(x)\left(\frac{\partial^2 y(x,t)}{\partial x^2}\right)^2 \mathrm{d}x = \frac{1}{2}\int_0^L [EI_0 - EI_c\delta(x-x_c)]\left(\frac{\partial^2 y(x,t)}{\partial x^2}\right)^2 \mathrm{d}x, \tag{3}$$

$$W_c = \int_0^L y(x,t)c\,\frac{\partial y(x,t)}{\partial t}\,\mathrm{d}x, \tag{4}$$

$$W = \int_0^L P(t)\delta(x-x_p)y(x,t)\,\mathrm{d}x. \tag{5}$$

Expressing the transverse displacement of the beam $y(x,t)$ in modal coordinates

$$y(x,t) = \sum_{i=1}^{n} Y_i(x)q_i(t), \tag{6}$$

where $Y_i(x)$ can be obtained from the assumed mode shapes. We have

$$T = \frac{1}{2}\int_0^L \rho A\left[\sum_{i=1}^{n} Y_i(x)\dot{q}_i(t)\sum_{j=1}^{n} Y_j(x)\dot{q}_j(t)\right]\mathrm{d}x = \frac{1}{2}\sum_{i=1}^{n}\sum_{j=1}^{n}\dot{q}_i(t)m_{ij}\dot{q}_j(t), \tag{7}$$

$$\begin{aligned} U &= \frac{1}{2}\int_0^L [EI_0 - EI_c\delta(x-x_c)]\left(\sum_{i=1}^{n} Y''_i(x)q_i(t)\sum_{j=1}^{n} Y''_j(x)q_j(t)\right)\mathrm{d}x \\ &= \frac{1}{2}\int_0^L EI_0\sum_{i=1}^{n} Y''_i(x)q_i(t)\sum_{j=1}^{n} Y''_j(x)q_j(t)\,\mathrm{d}x \\ &\quad -\frac{1}{2}\int_0^L EI_c\delta(x-x_c)\sum_{i=1}^{n} Y''_i(x)q_i(t)\sum_{j=1}^{n} Y''_j(x)q_j(t)\,\mathrm{d}x \\ &= \frac{1}{2}\sum_{i=1}^{n}\sum_{j=1}^{n} q_i(t)k_{ij}q_j(t) - \frac{1}{2}\sum_{i=1}^{n}\sum_{j=1}^{n} q_i(t)k'_{ij}q_j(t), \end{aligned} \tag{8}$$

$$W_c = \int_0^L c\sum_{i=1}^{n} Y_i(x)q_i(t)\sum_{j=1}^{n} Y_j(x)\dot{q}_j(t)\,\mathrm{d}x = \sum_{i=1}^{n}\sum_{j=1}^{n} q_i(t)c_{ij}\dot{q}_j(t), \tag{9}$$

$$W = \int_0^L P(t)\delta(x-x_p)\sum_{i=1}^{n} Y_i(x)q_i(t)\,\mathrm{d}x = \sum_{i=1}^{n} P(t)Y_i(x_p)q_i(t) = \sum_{i=1}^{n} f_i(t)q_i(t) \tag{10}$$

and

$$m_{ij} = \int_0^L \rho A Y_i(x) Y_j(x)\,\mathrm{d}x, \quad k_{ij} = \int_0^L EI_0 Y_i''(x) Y_j''(x)\,\mathrm{d}x,$$

$$k_{ij}' = \int_0^L EI_c \delta(x - x_c) Y_i''(x) Y_j''(x)\,\mathrm{d}x = EI_c Y_i''(x_c) Y_j''(x_c),$$

$$c_{ij} = \int_0^L c Y_i(x) Y_j(x)\,\mathrm{d}x, \quad f_i(t) = P(t) Y_i(x_p).$$

Substituting Eqs. (7)–(10) into the Lagrange equation

$$\frac{\mathrm{d}}{\mathrm{d}t}\left(\frac{\partial T}{\partial \dot{q}}\right) - \frac{\partial T}{\partial q} + \frac{\partial U}{\partial q} - \frac{\partial W_c}{\partial q} = \frac{\partial W}{\partial q} \tag{11}$$

we obtain

$$\sum_{j=1}^{n} m_{ij}\ddot{q}_j(t) + \sum_{j=1}^{n} c_{ij}\dot{q}_j(t) + \sum_{j=1}^{n} (k_{ij} - k_{ij}')q_j(t) = f_i(t) \quad i = 1, 2, \ldots, n. \tag{12}$$

Writing Eq. (12) in matrix form

$$[M]\{\ddot{q}(t)\} + [C]\{\dot{q}(t)\} + ([K] - [K'])\{q(t)\} = \{F(t)\}, \tag{13}$$

where

$$[M] = \{m_{ij}, i = 1, 2, \ldots, n; j = 1, 2, \ldots, n\}, \quad [C] = \{c_{ij}, i = 1, 2, \ldots, n; j = 1, 2, \ldots, n\},$$

$$[K] = \{k_{ij}, i = 1, 2, \ldots, n; j = 1, 2, \ldots, n\}, \quad [K'] = \{k_{ij}', i = 1, 2, \ldots, n; j = 1, 2, \ldots, n\},$$

$$\{q(t)\} = \{q_1(t), q_2(t), \ldots, q_n(t)\}^{\mathrm{T}}, \quad \{F(t)\} = \{f_1(t), f_2(t), \ldots, f_n(t)\}^{\mathrm{T}}. \tag{14}$$

The modal responses $\ddot{q}$, $\dot{q}$, q of the beam can then be obtained by direct integration, say, with the Newmark method [23].

2.2. The assumed mode shapes

The general form of the vibration mode for a uniform Euler beam can be written as

$$Y(x) = A_1 \cos \beta x + A_2 \sin \beta x + A_3 \cosh \beta x + A_4 \sinh \beta x, \tag{15}$$

where A_1, A_2, A_3, A_4 are constants and β is a frequency parameter. The vibration modes for an Euler beam with simply supported ends are obtained as

$$Y_i(x) = A_2 \sin \frac{\mathrm{i}\pi x}{L}. \tag{16}$$

It is noted that the effect of the crack on the vibration modes is very small [24] and it is not considered in this work.

2.3. Accuracy of the crack model

To validate the proposed crack model, the fundamental frequencies of the beam with the proposed crack model are compared with the results by Fernandez-Saez et al. [24]. They proposed a simplified method of evaluating the fundamental frequency for the bending vibrations of cracked Euler–Bernoulli beams with the crack in a beam modeled as an elastic spring. A closed form solution on the fundamental frequency was given for the simply supported cracked beam.

A 30 m long simply supported Euler–Bernoulli beam with an open crack at 4 m from the left support is studied. The parameters of the beam are: $\rho A = 5.0 \times 10^3\,\mathrm{kg/m}$, $E = 5 \times 10^{10}\,\mathrm{N/m^2}$, $L = 30\,\mathrm{m}$, $b = 0.6\,\mathrm{m}$, and $h_0 = 1.0\,\mathrm{m}$. Fig. 2 shows the variation of the ratio of fundamental frequency with crack to the original frequency with no crack from different ratio of crack depth. The results from both models are close to each other except for those from midspan, with the present model giving a slightly larger difference from those by Fernandez-Saez et al. [24].

Sinha et al. [25] proposed an open crack model in an Euler–Bernoulli beam element with a modified local flexibility of the beam in the vicinity of the crack. The same beam for the above study is investigated here with an excitation force of $f(t) = 40,000[1 + 0.1\sin(10\pi t) + 0.05\sin(40\pi t)]\ N$ applied at 7 m from the left support. The crack is at 4 m from the left support with 0.25 m depth. The displacement responses at the $\frac{1}{4}$ span and the middle point of the cracked beam were compared with the existing solution [25] as shown in Fig. 3. The responses obtained from both models are very close to each other indicating the accuracy of the proposed model.

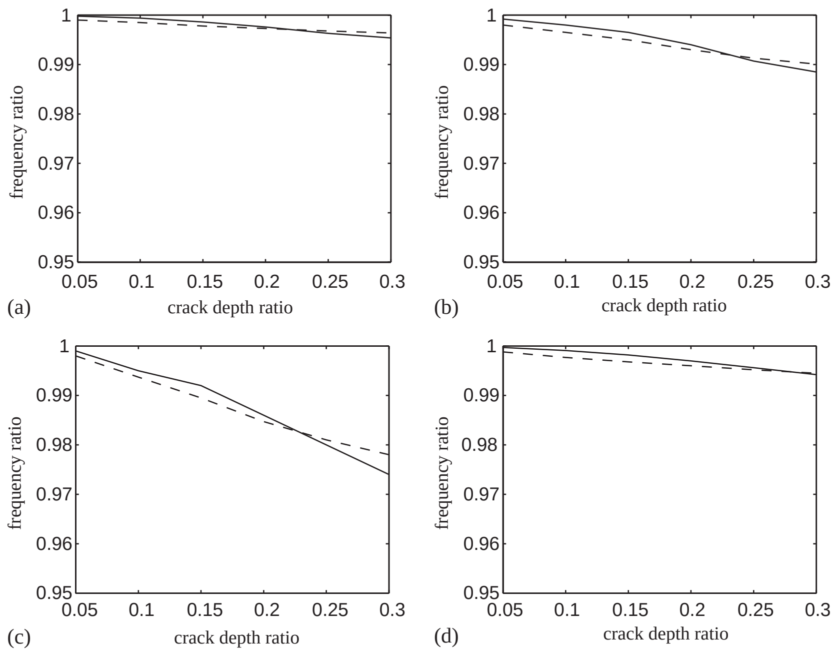

Fig. 2. The variation of the fundamental frequency corresponding to different crack location (—,[24], proposed, (a) $xc = 4\,\mathrm{m}$, (b) $xc = 7\,\mathrm{m}$, (c) $xc = 15\,\mathrm{m}$, (d) $xc = 25\,\mathrm{m}$.

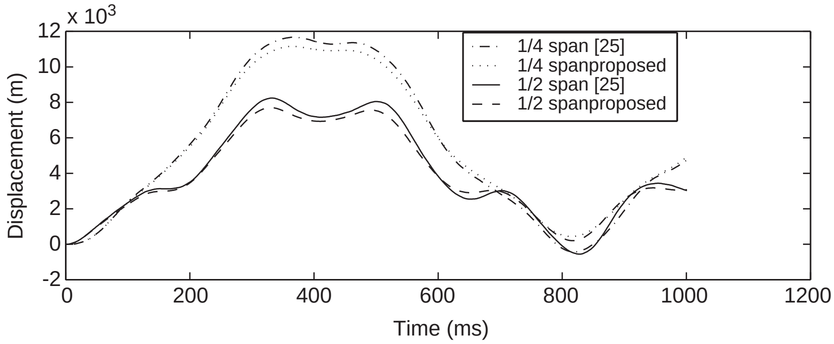

Fig. 3. The displacement responses of cracked beam for different crack model.

3. Inverse problem

3.1. Identification from measured displacements

Expressing the measured displacements $y(x_m, t)$ in modal coordinates

$$y(x_m, t) = \sum_{i=1}^{N} Y_i(x)q_i(t) \quad (m = 1, 2, \ldots, N_m), \tag{17}$$

where N_m is the number of measurement locations; $\{y(x_m, t),\ m = 1, 2, \ldots, N_m\}$ are the displacements at x_m. Eq. (17) can be re-written as

$$\{y\}_{N_m \times 1} = [Y]_{N_m \times N}\{q\}_{N \times 1}, \tag{18}$$

where $\{y\}_{N_m \times 1}$ is the vector of displacements at N_m measurement locations. The vector of generalized coordinates can be written using the least-squares pseudo-inverse as

$$\{q\}_{N \times 1} = ([Y]^{\mathrm{T}}_{N \times N_m}[Y]_{N_m \times N})^{-1}[Y]^{\mathrm{T}}_{N \times N_m}\{y\}_{N_m \times 1}. \tag{19}$$

The modal velocity and acceleration of the beam responses can be obtained from Eq. (19) by numerical methods. However, if the central difference method is used to calculate the modal velocity and acceleration, it will lead to large approximation error. Therefore the generalized orthogonal polynomial [26] is used to model the displacement so as to avoid the approximation error,

$$y(x_j, t) = \sum_{i}^{Nf} a_i T_i(t), \tag{20}$$

where $y(x_j, t)$ is the approximated displacement at the jth measuring point. The velocity and acceleration are then approximated by the first and second derivatives of the orthogonal polynomial. The orthogonal polynomial used in this work is shown in Appendix A.

Writing in matrix form, we have,

$$\{y\}_{N_m\times 1} = [A]_{N_m\times Nf}\{T\}_{Nf\times 1}, \quad \{\dot{y}\}_{N_m\times 1} = [A]_{N_m\times Nf}\{\dot{T}\}_{Nf\times 1},$$
$$\{\ddot{y}\}_{N_m\times 1} = [A]_{N_m\times Nf}\{\ddot{T}\}_{Nf\times 1}, \tag{21}$$

where $[A]_{N_m\times Nf}$, $\{T\}_{Nf\times 1}$, $\{\dot{T}\}_{Nf\times 1}$, $\{\ddot{T}\}_{Nf\times 1}$ are the coefficient matrix of the polynomial, the orthogonal polynomial matrix, the first and second derivatives of the orthogonal polynomial variable matrix respectively. N_f is the order of the orthogonal polynomial. The coefficient matrix $[A]$ can be obtained by the least-squares method from Eq. (21) as

$$[A]_{N_m\times Nf} = \{y\}_{N_m\times 1}\{T\}^{\mathrm{T}}_{1\times Nf}(\{T\}_{Nf\times 1}\{T\}^{\mathrm{T}}_{1\times N_f})^{-1}. \tag{22}$$

Substituting matrix $[A]$ into Eq. (21), we can get $\{\dot{y}\}$ and $\{\ddot{y}\}$. And substituting $\{y\}$, $\{\dot{y}\}$, $\{\ddot{y}\}$ and the derivatives of $\{T\}$ into Eq. (19), we can obtain the modal displacement q, modal velocity $\dot{q}$ and modal acceleration $\ddot{q}$. Substituting further q, $\dot{q}$ and $\ddot{q}$ into Eq. (13), we have

$$K'q = M\ddot{q} + C\dot{q} + Kq - F(t). \tag{23}$$

The elements of matrix K' are obtained as follows with the first-order approximation

$$k'_{ij} = EI_c Y''_i(x_c)Y''_j(x_c) \approx \frac{Ebh_0^2h_c}{4}\, Y''_i(x_c)Y''_j(x_c). \tag{24}$$

The inverse problem here is how to find the crack location and the crack depth from Eq. (23). When at time t_i, we have the following from Eqs. (23) and (24).

$$[K']\begin{Bmatrix} q_1(t_i) \\ q_2(t_i) \\ \vdots \\ q_n(t_i) \end{Bmatrix} = [M]\begin{Bmatrix} \ddot{q}_1(t_i) \\ \ddot{q}_2(t_i) \\ \vdots \\ \ddot{q}_n(t_i) \end{Bmatrix} + [C]\begin{Bmatrix} \dot{q}_1(t_i) \\ \dot{q}_2(t_i) \\ \vdots \\ \dot{q}_n(t_i) \end{Bmatrix} + [K]\begin{Bmatrix} q_1(t_i) \\ q_2(t_i) \\ \vdots \\ q_n(t_i) \end{Bmatrix} - \begin{Bmatrix} f_1(t_i) \\ f_2(t_i) \\ \vdots \\ f_n(t_i) \end{Bmatrix}. \tag{25}$$

Rewriting Eq. (25), and let

$$J(x_c,h_c) = [K']\begin{Bmatrix} q_1(t_i) \\ q_2(t_i) \\ \vdots \\ q_n(t_i) \end{Bmatrix} - \left[[M]\begin{Bmatrix} \ddot{q}_1(t_i) \\ \ddot{q}_2(t_i) \\ \vdots \\ \ddot{q}_n(t_i) \end{Bmatrix} + [C]\begin{Bmatrix} \dot{q}_1(t_i) \\ \dot{q}_2(t_i) \\ \vdots \\ \dot{q}_n(t_i) \end{Bmatrix} + [K]\begin{Bmatrix} q_1(t_i) \\ q_2(t_i) \\ \vdots \\ q_n(t_i) \end{Bmatrix} - \begin{Bmatrix} f_1(t_i) \\ f_2(t_i) \\ \vdots \\ f_n(t_i) \end{Bmatrix}\right] \tag{26}$$

or

$$J(x_c,h_c) = A(p) - d, \tag{27}$$

where $J(x_c,h_c)$ is an error vector, and $A(p)$ represents the first term of the right-hand side of Eq. (26), and d represents the second term, the vector p contains the unknown crack location and depth parameters.

Now the problem becomes a nonlinear optimization problem with two unknown parameters: the crack depth h_c and the location x_c. This is equivalent to minimizing the error function

$$\min \|J(x_c, h_c)\|^2 = \min \|A(p) - d\|^2. \tag{28}$$

Like many inverse problems, this is an ill-conditioned problem, and regularization method is adopted to provide bounds to the solution. A regularization term λ is introduced into the right-hand side of Eq. (28)

$$\min \|J(x_c, h_c)\|^2 = \min\{\|A(p) - d\|^2 + \lambda\|p - p_0\|^2\}, \tag{29}$$

where $\lambda > 0$ and p_0 is the vector containing the a priori information on the crack location and depth at time t_i.

The following strategy is proposed to locate approximately the crack. It is known that when the identified crack location does not match the real location, the identified crack depth exhibits large fluctuations due to ill-conditioning in the solution. Therefore, the variance of the identified crack depth time history from using different initial crack location in the calculation is taken as an indicator. The correct initial guess on the crack location should correspond to the smallest variance in the identified crack depth time history.

The crack identification can be realized through the following steps: the mode shape $Y_i(x)$ are obtained from Eq. (16). The modal displacement q, modal velocity $\dot{q}$ and modal acceleration $\ddot{q}$ are computed from Eq. (21). Then by minimizing the error function J, we can get the crack location x_c and the crack depth h_c.

3.2. Identification from measured strains

The strain at the bottom of a rectangular beam with depth h_0 can be expressed in terms of the generalized coordinates as

$$\varepsilon(x_m, t) = -\frac{h_0}{2} \sum_{i=1}^{N} Y''(x_m) q_i(t) \quad (m = 1, 2, \ldots, N_m), \tag{30}$$

where N_m is the number of measurement locations; $\{\varepsilon(x_m, t), m = 1, 2, \ldots, N_m\}$ are the strains at x_m. Eq. (30) can be written as

$$\{\varepsilon\}_{N_m \times 1} = -\frac{h_0}{2}[Y'']_{N_m \times N}\{q\}_{N \times 1}, \tag{31}$$

where $\{\varepsilon\}_{N_m \times 1}$ is the vector of strains at N_m measurement locations. Again the strain can be approximated by the orthogonal polynomial $T(t)$ as

$$\varepsilon(x_j, t) = \sum_{i}^{Nf} a_i T_i(t), \tag{32}$$

where $\varepsilon(x_j, t)$ is the strain at the jth measuring point. The rest of the computation in the identification is similar to those for identification from measured displacements mentioned above.

4. Multiple cracks identification

The proposed formulation for single crack can be extended to identify N_c single-sided transverse cracks in the beam, and Eq. (1) becomes

$$\rho A \frac{\partial^2 y(x,t)}{\partial t^2} + c\frac{\partial y(x,t)}{\partial t} + \left(EI_0 - \sum_{k=1}^{Nc} E(I_c)_k \delta(x-(x_c)_k) \right) \frac{\partial^2}{\partial x^2}\left(\frac{\partial^2 y(x,t)}{\partial x^2}\right) = P(t)\delta(x-x_p). \tag{33}$$

Matrix K' in Eq. (14) becomes

$$K' = \sum_{k=1}^{Nc} (k'_{ij})_k \quad (i=1,2,\ldots,n; j=1,2,\ldots,n), \tag{34}$$

where $(k'_{ij})_k$ is the matrix k'_{ij} in Eq. (24) for the kth crack, and Eq. (25) becomes

$$\frac{Ebh_0^2}{4}\begin{bmatrix} \sum_{k=1}^{Nc} Y_1''((x_c)_k)Y_1''((x_c)_k)h_{ck} & \sum_{k=1}^{Nc} Y_1''((x_c)_k)Y_2''((x_c)_k)h_{ck} & \cdots & \sum_{k=1}^{Nc} Y_1''((x_c)_k)Y_n''((x_c)_k)h_{ck} \\ \sum_{k=1}^{Nc} Y_2''((x_c)_k)Y_1''((x_c)_k)h_{ck} & \sum_{k=1}^{Nc} Y_2''((x_c)_k)Y_2''((x_c)_k)h_{ck} & \cdots & \sum_{k=1}^{Nc} Y_2''((x_c)_k)Y_n''((x_c)_k)h_{ck} \\ \vdots & \vdots & \vdots & \vdots \\ \sum_{k=1}^{Nc} Y_n''((x_c)_k)Y_1''((x_c)_k)h_{ck} & \sum_{k=1}^{Nc} Y_n''((x_c)_k)Y_2''((x_c)_k)h_{ck} & \cdots & \sum_{k=1}^{Nc} Y_n''((x_c)_k)Y_n''((x_c)_k)h_{ck} \end{bmatrix}$$

$$\times \begin{Bmatrix} q_1(t_i) \\ q_2(t_i) \\ \vdots \\ q_n(t_i) \end{Bmatrix} = [M]\begin{Bmatrix} \ddot{q}_1(t_i) \\ \ddot{q}_2(t_i) \\ \vdots \\ \ddot{q}_n(t_i) \end{Bmatrix} + [C]\begin{Bmatrix} \dot{q}_1(t_i) \\ \dot{q}_2(t_i) \\ \vdots \\ \dot{q}_n(t_i) \end{Bmatrix} + [K]\begin{Bmatrix} q_1(t_i) \\ q_2(t_i) \\ \vdots \\ q_n(t_i) \end{Bmatrix} - \begin{Bmatrix} f_1(t_i) \\ f_2(t_i) \\ \vdots \\ f_n(t_i) \end{Bmatrix}. \tag{35}$$

The crack identification formulation will be similar to the single-crack identification, and both the displacement and strain measurements can be used to identify multiple cracks in the beam.

5. Simulation results

5.1. Single-crack identification

A 30 m long simply supported Euler–Bernoulli beam with an open crack is studied. The first six natural frequencies of the uncracked beam are: 1.23, 4.94, 11.11, 19.75, 30.86 and 44.43 Hz. The damping ratios for these modes are all equal to 0.02. The external exciting force is

$$f(t) = 40,000[1 + 0.1\sin(10\pi t) + 0.05\sin(40\pi t)]N$$

and is applied at 7 m from the left support. The dynamic components of the force are close to the second and fourth modal frequencies of the beam. The parameters of the beam are: $\rho A = 5.0 \times 10^3$ kg/m, $E = 5 \times 10^{10}$ N/m^2, $L = 30$ m, $b = 0.6$ m, and $h_0 = 1.0$ m. White noise is added to the calculated displacements and strains to simulate the polluted measurements as follows

$$y = y_{\text{calculated}} + E_p * N_{\text{oise}} * \text{var}(y_{\text{calculated}}),$$

$$\varepsilon = \varepsilon_{\text{calculated}} + E_p * N_{\text{oise}} * \text{var}(\varepsilon_{\text{calculated}}),$$

where y and ε are the vectors of polluted displacement and strain respectively, E_p is the noise level, N_{oise} is a standard normal distribution vector with zero mean and unit standard deviation; var($\bullet$) is the variance of the time history, $y_{\text{calculated}}$ and $\varepsilon_{\text{calculated}}$ are the vectors of calculated displacement and strain. Noise levels (0%, 5% and 10%) are studied in this paper. In the numerical simulation, the crack locates at 4 m from the left support with the crack depth h_c equals 0.25 m.

The first three modes are used in the calculation. Measured strains at $\frac{1}{4}L$, $\frac{1}{2}L$ and $\frac{3}{4}L$ are used in the identification. The sampling frequency is 100 Hz, which is larger than two times the highest frequency of interest at 44.43 Hz.

Fig. 4 shows the plot of variance of the identified crack depth time history against the initial crack location. The crack depth is taken as zero in the search for the crack location. The optimal regularization parameter λ was found different for different initial crack location, and it is taken equal to 200 for the preparation of Fig. 4. The results confirm that the smallest variance corresponds to the correct crack location. In fact a wide range of λ from 20 to 200 gives results similar to Fig. 4.

The initial crack location is then set at 4 m as from Fig. 4 with an initial zero crack depth. The regularization parameter is plotted against the variance of the identified crack location in Fig. 5. The variance gradually increases with a reduction in the parameter until a point where there is a

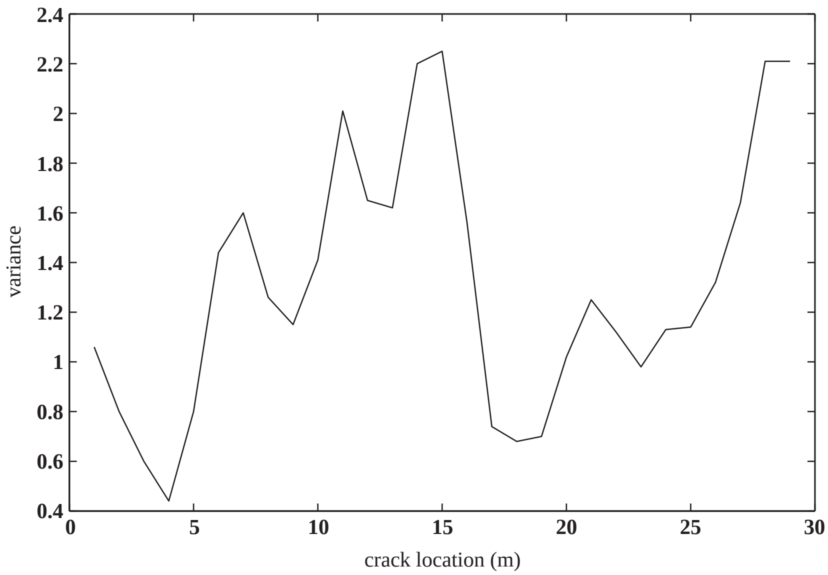

Fig. 4. The variance of the identified crack location (5% noise).

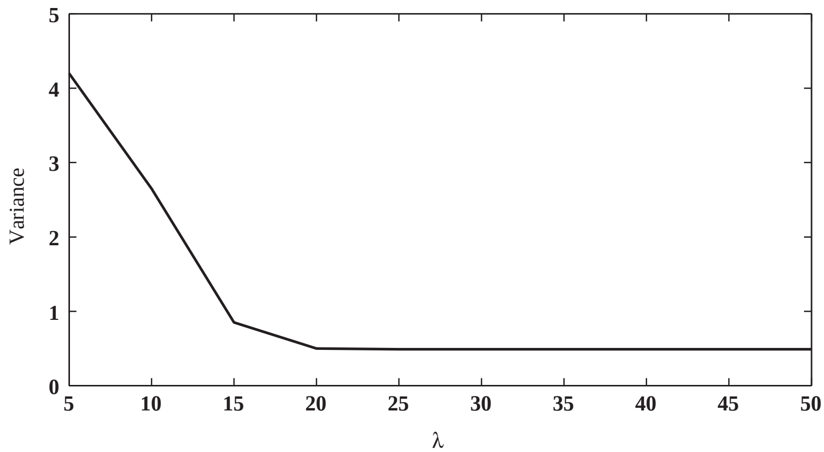

Fig. 5. The optimal regularization parameter (corresponding to crack location at 4 m and 5% noise).

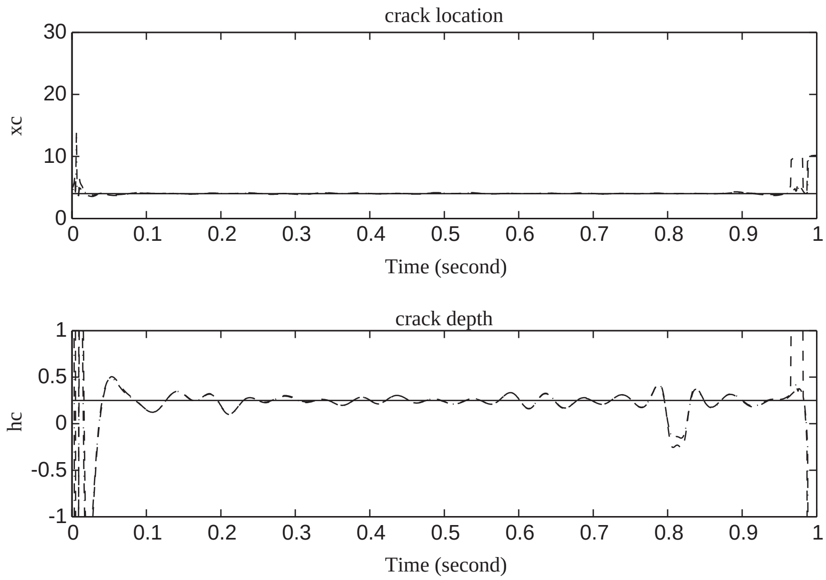

Fig. 6. Crack identification from different noise level (—, true; ···, no noise; ---, 10% noise).

sudden jump in the variance. The value of λ corresponds to the point before this sudden jump ($\lambda = 20$) is taken as the optimal regularization parameter.

Fig. 6 shows the identified results from measured strains without any noise and with 10% noise respectively. There is little difference in the identified crack depth time histories from both cases. The polluted measurements have been approximated with orthogonal polynomial functions with 20 terms, and the velocity and accelerations subsequently obtained by direct differentiating the functions are compared with those from the measurements in Fig. 7, and they are found matching each other very well. Larger errors are only found in the accelerations.

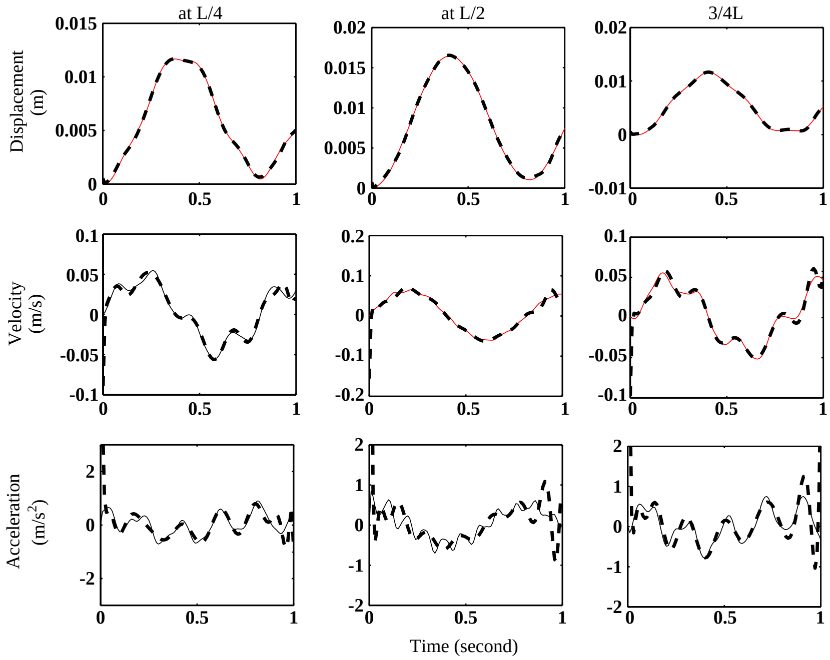

Fig. 7. Responses at the measuring points (—, from simulation; - - -, from orthogonal function).

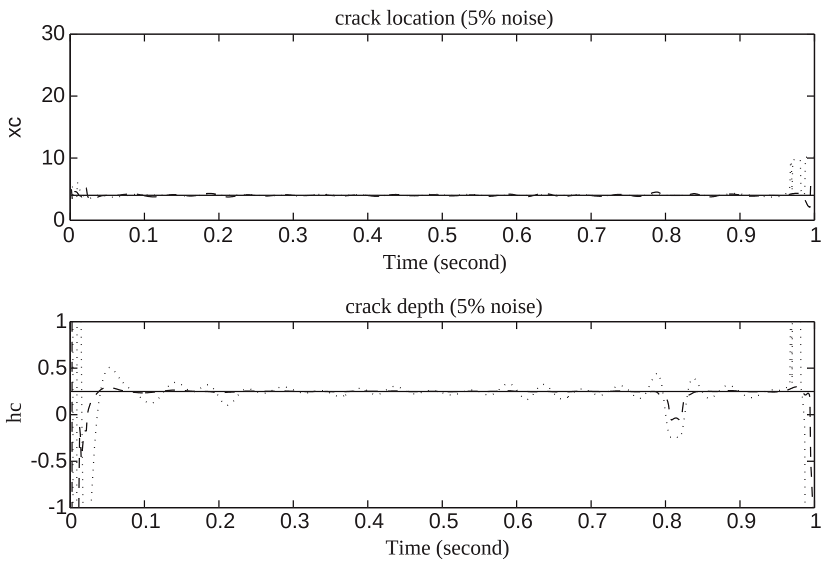

Fig. 8. Crack identification from 3 and 6 modes (—, true; $\cdots$, 3 modes; - - -, 6 modes).

The effect of modal truncation on the identification is also studied. Fig. 8 shows the identified results from using the first three and six modes. And the number of measuring points is taken equal to the number of vibration modes with the measuring points evenly distributed on the beam.

The sampling frequency is 100 Hz, and 5% noise level is included in measurement. It can be seen from the figure that the identification accuracy increases with increasing number of modes in the identification, but the curves obtained from using only three modes are still varying close to the true curves.

Large fluctuations are found in the identified crack depth within the first and final quarters of the time history in all the above cases. This can be explained by observing the acceleration and velocity obtained from the orthogonal polynomial functions in Fig. 7. Errors are found in these time derivatives near the beginning and end of the time histories while those in the middle halve are well approximated by the polynomials. This is the major source of error in the identification and is due to the discontinuity of the time responses with the excitation force. The identification error is found to decrease when more modes are used.

5.2. Multi-cracks identification

The same simply supported Euler–Bernoulli beam with three open cracks is studied. The crack locations are at 4, 14 and 24 m from the left support. The open crack depths are arbitrarily taken as $h_{c1} = 0.2\,\mathrm{m}$, $h_{c2} = 0.25\,\mathrm{m}$ and $h_{c3} = 0.2\,\mathrm{m}$.

The first 6 modes and 6 displacement measurements are used in the identification, and 5% noise is included. The measuring points are evenly distributed on the beam, and the sampling frequency is 100 Hz. The same sinusoidal excitation force as for single-crack identification is used in this study. The strategy for searching the optimal location for the single-crack identification is not applicable for multiple cracks because of the existence of numerous local minima in the search for the global minimum variance. This strategy assumes that the desired locations are close to the nominal initial values and that there are no spurious solutions in the neighborhood of the correct solution. These assumptions are not valid in this case because the nominal initial values on the locations are not known. Hjelmstad [27] has used a random starting point scheme in conjunction with the objective minimization algorithm to find all the multiple minima of the parameter estimation problem. Pothisiri and Hjelmstad [28] have also proposed a method to find a near-optimal measurement set for parameter estimation. Both of these methods could be applied to the present problem to find solutions on the initial crack locations.

In this paper the true locations of the cracks are included in the identification, and the optimal regularization parameter is 100 in this study. Fig. 9 shows the identification results on the three cracks, the first two are found almost overlapping with the true curve while the third one varies around the true curve. Large fluctuations are found at both ends of the time history similar to those found in the single-crack identification.

5.3. Crack identification from an impulsive force

A periodic impulsive force is applied on the same beam as for the above study with a period of 1 s, and the duration of the force is 0.1 s. The magnitude of the force is 9500 N simulating the impact excitation produced by a 125 kg weight free falling for 1 m on the beam. The effect of the falling mass after the impact is ignored. The force is applied at 7 m from the left support and it can

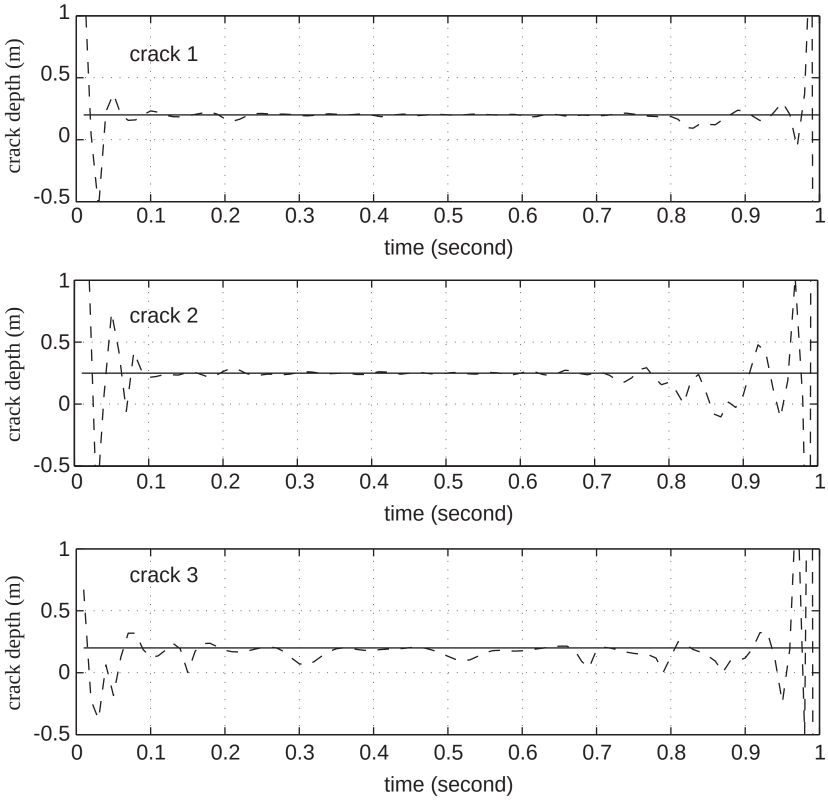

Fig. 9. Identified crack depth for the three cracks (5% noise) (—, true; - - -, identified).

be expressed in the following form:

$$f(t) = \begin{cases} 190,000(t - 0.05) & 0.05 \leqslant t \leqslant 0.1, \\ 190,000(0.15 - t) & 0.1 \leqslant t \leqslant 0.15. \end{cases}$$

A Fourier series is used to simulate the force, i.e.

$$f(t) = \alpha_0 + \sum_{k=1}^{\infty} \alpha_k \cos \frac{2k\pi t}{T} + \sum_{k=1}^{\infty} \beta_k \sin \frac{2k\pi t}{T},$$

where

$$\alpha_0 = \frac{1}{T} \int_0^T f(t)\,\mathrm{d}t,$$

$$\alpha_k = \frac{2}{T} \int_0^T f(t) \cos \frac{2k\pi t}{T}\,\mathrm{d}t \quad \text{and} \quad \beta_k = \frac{2}{T} \int_0^T f(t) \sin \frac{2k\pi t}{T}\,\mathrm{d}t.$$

Forty terms in the series are used to include the higher frequency components in the force. The crack location and crack depth are the same as for the single-crack identification. The

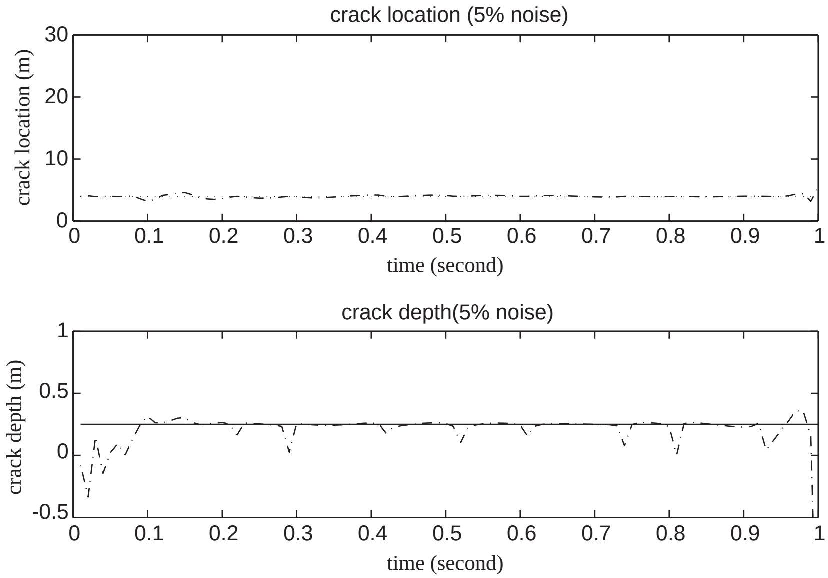

Fig. 10. Crack identification from impulsive force (—, true; - · - · -, identified).

Table 1
Comparison with existing method

	Single crack		Depth of crack (m)		
	Location (m)	Depth (m)	Crack 1	Crack 2	Crack 3
True value	4.0	0.25	0.20	0.25	0.20
Sinha et al. [25]	4.16/4%	0.31/24%	0.235/17.5%	0.21/−16%	0.237/17.5%
Proposed method	4.03/0.75%	0.23/−8%	0.195/−2.5%	0.254/1.6%	0.182/−9%

Note: •/• denotes the identified value and percentage of error.

regularization parameter is 20. The sampling frequency is 100 Hz, and the first 6 modes and 6 displacement measurements are used in the identification. Five percent noise is included in the identification. The measuring points are evenly distributed on the beam. Fig. 10 shows that the identified crack depth is close to the true one. Results not shown here indicate that the identified result is less dependent on the sampling rate. This is because the impulsive force consists of a wide spectrum of frequency components as an excitation force, but the majority of the responses come from the first few modes of the structure which can be easily collected using a low sampling rate.

5.4. Comparison with existing method

The accuracy of identification results is compared with those from Sinha et al. [25] for the cases of single crack and multiple cracks under sinusoidal excitation and results from both methods are listed in Tables 1 and 2. Since the parameters are identified in a time series, the data obtained from averaging the identified values during the period 0.1–0.6 s are taken as the results. This is to avoid

Table 2
Experimental modal frequencies (Hz) of the cracked beam

Crack depth and location	Mode number				
	1	2	3	4	5
No crack	22.868	62.763	123.049	203.236	303.452
$h_c = 3\,\text{mm}$ at 1720 mm	22.797	62.622	122.559	202.271	302.490
$h_c = 6\,\text{mm}$ at 1720 mm	22.766	62.378	121.704	201.050	301.514
$h_c = 9\,\text{mm}$ at 1720 mm	22.766	61.890	119.995	198.486	299.500

the errors close to the beginning and end of the time histories due to the discontinuity of the time response with the excitation force. The propose method is found giving much better accuracy with 5% or 10% noise in the measurement than Sinha et al. without any measurement noise both in the location and crack depth. It is also noted that the crack parameters are identified in the time domain, and this means that the proposed method can be used to identify breathing cracks in the beam with time varying parameters.

6. Laboratory verification

Experimental results are used to verify the algorithm developed for the crack identification. The parameters of the test sample are: $L = 2.1\,\text{m}$, $b = 0.025\,\text{m}$, $h_0 = 0.019\,\text{m}$, $E = 2.07 \times 10^{11}\,\text{N/m}^2$, $\rho = 7.832 \times 10^3\,\text{kg/m}^3$. The crack is at 1.72 m from the left free end, and is created using a machine saw with 1.3 mm thick cutting blade. Five measured strains were used to identify the crack in the beam which were located at 0.6, 0.9, 1.1, 1.4 and 1.95 m from the left free end respectively. An impulsive force was applied with an impact hammer model B&K 8202 at 1.2 m from the left free end. The sampling frequency is 2000 Hz, and the data record time duration is 1 min. The data are re-sampled with a sampling frequency of 500 Hz in the identification in order to improve the computation efficiency. The first 5 natural frequencies of the intact and the damaged beam with the crack depth at 3, 6 and 9 mm are shown in Table 1. The frequencies do not change much with damage in the first two modes. Fig. 11 shows a sample of the impulsive force and the five measured strains when the crack depth is 6 mm. Two hammer hits were applied on the beam within this duration. It is noted that the measured strains from the beam are very small with a maximum of approximately 60μ at 1.1 m.

Fig. 12 shows the identified results for the different crack depths. The first 4 modes are used in the identification. And the regularization parameter λ is 100. Due to the limitation of the computer memory, only the first 7.0 s measured strains were used in the identification. The location of the crack can be obtained from a study of the variance of the identified results as what has been done in the simulation study. The identified crack depth time history fluctuates close to the true value of the time history for all the cases. The identified crack depth for 9 mm crack is more accurate than those with smaller depth. It is noted that these results comes from two hammer hits on the beam with very low level of dynamic responses. The identified results are

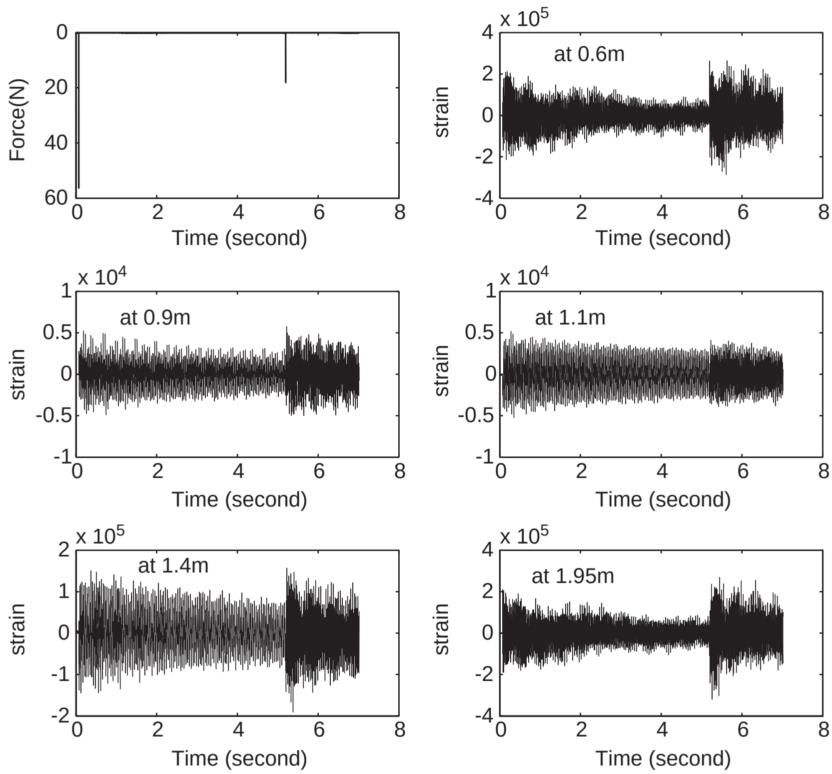

Fig. 11. The impulsive force and five measured strains.

believed to improve significantly with longer duration in the identification or if more hammer hits are included within the time duration of computation.

7. Conclusion

This paper includes the crack damage in the identification equation of a beam structure. A crack with a constant depth is modeled with a Dirac delta function, and a method is proposed to identify the open crack in beam structures based on dynamic measurements in time domain. Only several displacement or strain measurements and the first few modes are required in the crack identification. The method is based on modal superposition and optimization technique with regularization on the solution. Orthogonal polynomial function is used to approximate the measured strain or displacement for a practical application with noisy measurements. Computation simulations using sinusoidal and impulsive excitations on a beam with a single or multiple cracks show that the method is effective to identify cracks and is much more accurate than the method by Sinha et al. [25] from polluted measurements. Experimental results also show that a few hammer hits could be used as the excitation source for the single-crack identification.

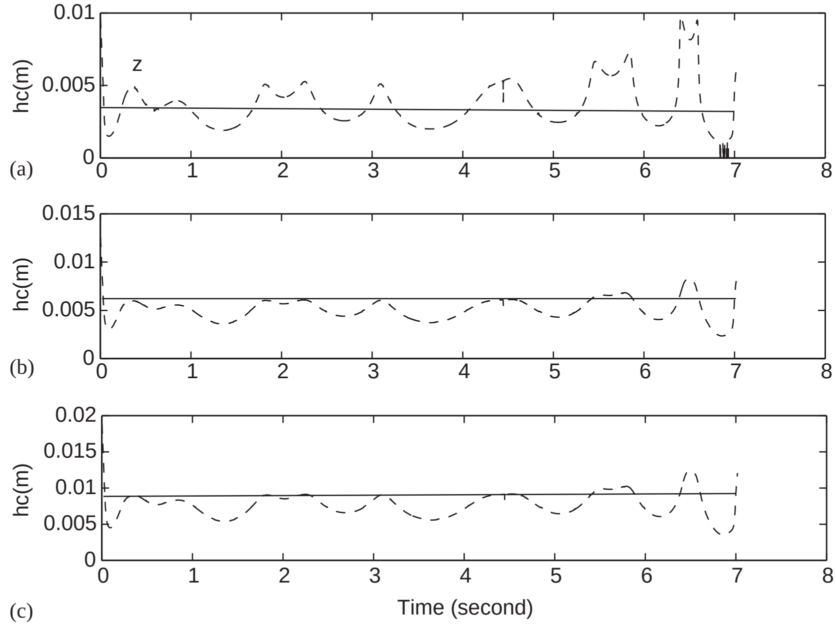

Fig. 12. Crack identification from measured strains: (a) $hc = 3\,\text{mm}$, (b) $hc = 6\,\text{mm}$, (c) $hc = 9\,\text{mm}$; (—, true; - - -, identified).

Acknowledgements

The work described in this paper was supported by a research grant from the Hong Kong Polytechnic University.

Appendix A. Generalized orthogonal polynomial function

$$T_1 = \frac{1}{\sqrt{\pi}},$$

$$T_2 = \sqrt{\frac{2}{\pi}}\left(\frac{2}{T}\,t - 1\right),$$

$$T_3 = \sqrt{\frac{2}{\pi}}\left(2\left(\frac{2}{T}\,t - 1\right)^2 - 1\right),$$

$$T_{j+1} = 2\left(\frac{2}{T}\,t - 1\right)T_j - T_{j-1}.$$

References

[1] A. Ibrahim, F. Ismail, H.K. Martin, Identification of fatigue cracks from vibrating testing, *Journal of Sound and Vibration* 140 (1990) 305–317.
[2] S.M. Cheng, A.S.J. Swamidas, X.J. Wu, W. Wallace, Vibrational response of a beam with a breathing crack, *Journal of Sound and Vibration* 225 (1999) 201–208.
[3] P.F. Rizos, N. Aspragathos, A.D. Dimarogonas, Identification of crack location and magnitude in a cantilever beam from the vibration modes, *Journal of Sound and Vibration* 138 (1990) 381–388.
[4] R.D. Adams, P. Cawley, C.J. Pye, B.J. Stone, A vibration technique for non-destructively assessing the integrity of structures, *Journal of Mechanical Engineering Science* 20 (1978) 93–100.
[5] W.M. Ostachowich, M. Krawczuk, Analysis of the effect of cracks on the natural frequencies of a cantilever beam, *Journal of Sound and Vibration* 150 (1991) 191–201.
[6] P.G. Kirshmer, The effect of discontinuities on the natural frequency of the beam, in: *Proceedings of ASTM*, vol. 44, 1994, pp. 897–904.
[7] W.T. Thomson, Vibration of slender bars with discontinuities in stiffness, *Journal of Applied Mechanics* 16 (1949) 203–207.
[8] H.J. Petroski, Simple static and dynamic models for cracked elastic beam, *International Journal of Fracture* 17 (1981) R71–R76.
[9] A. Joshi, B.S. Madhusudhan, A unified approach to free vibration of locally damaged beams having various homogeneous boundary conditions, *Journal of Sound and Vibration* 147 (1991) 475–488.
[10] M.H.H. Shen, C. Pierre, Free vibration of beam with a single-edged crack, *Journal of Sound and Vibration* 170 (1994) 237–259.
[11] S. Christides, A.D.S. Barr, One-dimensional theory of cracked Bernoulli–Euler beam, *International Journal of Mechanical Sciences* 26 (1984) 639–648.
[12] I. Ballo, Non-linear effects of vibration of a continuous transverse cracked slender shaft, *Journal of Sound and Vibration* 217 (2) (1998) 321–333.
[13] T.G. Chondros, A.D. Dimarogonas, J. Yao, A continuous cracked beam vibration theory, *Journal of Sound and Vibration* 215 (1) (1998) 17–34.
[14] J.A. Brandon, O.N.L. Abraham, Counter-intuitive quasi-periodic motion in the autonomous vibration of cracked Timoshenko beams, *Journal of Sound and Vibration* 185 (3) (1998) 415–430.
[15] P. Cawley, R.D. Adams, The location of defects in structures from measurement of natural frequencies, *Journal of Strain Analysis* 14 (1979) 49–57.
[16] A. Messina, I.A. Jones, E.J. Williams, Damage detection and localization using natural frequency change, in: *14th International Modal Analysis Conference*, Orlando, FL, 1996, pp. 67–76.
[17] A. Messina, E.J. Williams, T. Contursi, Structural damage detection by sensitivity and statistical-based method, *Journal of Sound and Vibration* 216 (5) (1998) 791–808.
[18] A.K. Pandey, M. Biswas, M.M. Samman, Damage detection from changes in mode shapes, *Journal of Sound and Vibration* 145 (2) (1991) 321–332.
[19] Z.Y. Shi, S.S. Law, Structural damage detection from modal strain energy change, *Journal of Engineering Mechanics* 126 (12) (2002) 1216–1223.
[20] J. Cattarius, D.J. Inman, Time domain analysis for damage detection in smart structures, *Mechanical Systems and Signal Processing* 11 (3) (1997) 409–423.
[21] C.G. Koh, B. Hong, C.Y. Liaw, Parameter identification of large structural systems in time domain, *Journal of Structural Engineering* ASCE 126(8) (2000) 957–963.
[22] L. Majumder, C.S. Manohar, A time domain approach for damage detection in beam structures using vibration data with a moving oscillator as an excitation source, *Journal of Sound and Vibration* 268 (4) (2003) 699–716.
[23] N.W. Newmark, A method of computation for structural dynamics, *Journal of Engineering Mechanics Division* ASCE 85(3) (1959) 67–94.
[24] J. Fernandez-Saez, L. Rubio, C. Navarro, Approximate calculation of the fundamental frequency for bending vibrations of cracked beams, *Journal of Sound and Vibration* 225 (2) (1999) 345–352.

[25] J.K. Sinha, M.I. Friswell, S. Edwards, Simplified models for the location of cracks in beam structures using measured vibration data, *Journal of Sound and Vibration* 251 (1) (2002) 13–38.
[26] S.S. Law, X.Q. Zhu, Study on different beam models in moving force identification, *Journal of Sound and Vibration* 234 (2000) 661–679.
[27] K.D. Hjelmstad, On the uniqueness of modal parameter estimation, *Journal of Sound and Vibration* 192 (1996) 581–598.
[28] T. Pothisiri, K.D. Hjelmstad, Strategy for finding a near-optimal measurement set for parameter estimation from modal response, *Journal of Sound and Vibration* 257 (1) (2002) 89–106.